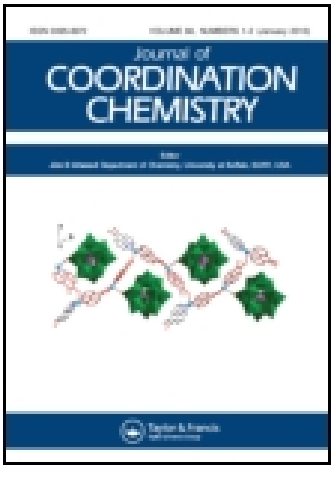

Journal of Coordination Chemistry
Publication details, including instructions for authors and subscription information:
http://www.tandfonline.com/loi/gcoo20

Syntheses, crystal structures, spectral studies, and DFT calculations of two new square planar Ni(II) complexes derived from pyridoxal-based Schiff base ligands

Senjuti Mandal[a], Sudipta Chatterjee[b], Ritwik Modak[a], Yeasin Sikdar[a], Barnali Naskar[a] & Sanchita Goswami[a]
[a] Department of Chemistry, University of Calcutta, Kolkata, India
[b] Department of Chemistry, Serampore College, Hooghly, India
Accepted author version posted online: 07 Feb 2014.Published online: 06 Mar 2014.

To cite this article: Senjuti Mandal, Sudipta Chatterjee, Ritwik Modak, Yeasin Sikdar, Barnali Naskar & Sanchita Goswami (2014) Syntheses, crystal structures, spectral studies, and DFT calculations of two new square planar Ni(II) complexes derived from pyridoxal-based Schiff base ligands, Journal of Coordination Chemistry, 67:4, 699-713, DOI: 10.1080/00958972.2014.890190

To link to this article: http://dx.doi.org/10.1080/00958972.2014.890190

Journal of Coordination Chemistry, 2014
Vol. 67, No. 4, 699–713, http://dx.doi.org/10.1080/00958972.2014.890190

Syntheses, crystal structures, spectral studies, and DFT calculations of two new square planar Ni(II) complexes derived from pyridoxal-based Schiff base ligands

SENJUTI MANDAL†, SUDIPTA CHATTERJEE‡, RITWIK MODAK†, YEASIN SIKDAR†, BARNALI NASKAR† and SANCHITA GOSWAMI*†

†Department of Chemistry, University of Calcutta, Kolkata, India
‡Department of Chemistry, Serampore College, Hooghly, India

(*Received 13 August 2013; accepted 27 November 2013*)

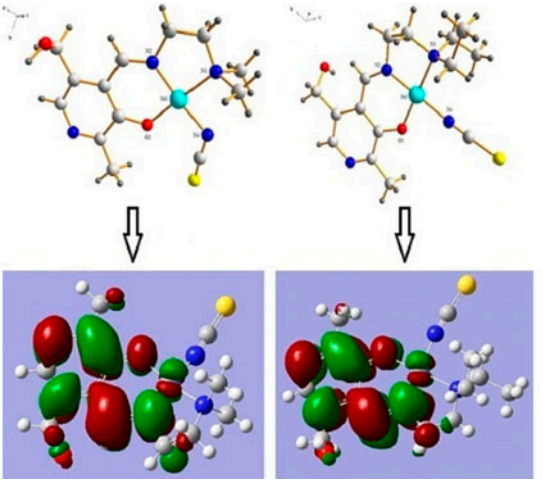

Two new square planar Ni(II) complexes, [Ni(L^1)SCN] (**1**) and [Ni(L^2)SCN] (**2**) are synthesized from pyridoxal-based Schiff base ligands and structurally characterized. DFT calculations are also done to establish their optimized electronic structures.

Two new complexes based on a Schiff base derived from pyridoxal N,N-dimethylethylenediamine (HL^1) and N,N-diethylethylenediamine (HL^2), [Ni(L^1)SCN] (**1**) and [Ni(L^2)SCN] (**2**), have been synthesized and structurally characterized by single-crystal X-ray diffraction along with other physical techniques, including elemental analyses, IR spectra, cyclic voltammetry, UV–vis, and luminescence studies. X-ray studies suggest that in both the complexes nickel lies in a slightly distorted square planar environment occupied by the tridentate ONN ligand and an isothiocyanate moiety. Density functional theory computations have been carried out to characterize the complexes.

Keywords: Square planar Ni(II); Crystal structures; DFT

*Corresponding author. Email: sgchem@caluniv.ac.in

1. Introduction

The biologically active form of vitamin B_6, pyridoxal-5-phosphate (PLP), is a versatile enzyme cofactor responsible for amino acid metabolism in all organisms from bacteria to human [1–3]. From a mechanistic standpoint, a PLP mediated transamination most likely begins with the formation of a Schiff base at the N-terminus [1, 4]. Hence, the study of metal complexes derived from pyridoxal Schiff bases will be important for understanding of the mechanism of action of pyridoxal *in vivo*, and also for developing new bioactive compounds [5, 6]. In our previous work, we characterized a copper(II)-pyridoxal complex and studied its fluorescence behavior, which showed that the fluorescence intensity of the pyridoxal ligand was efficiently and selectively quenched by Cu(II) [7].

Mononuclear Ni(II) complexes play an important role in modeling metallo-protein sites [8]. Bio-inspired nickel coordination chemistry has flourished and the resulting synthetic models for the active sites of nickel-containing enzymes have been reviewed [9]. Nickel is present in the environment originating from natural and anthropogenic sources and also important in modern industry [9]. Nickel may also be a serious enemy in human organism and a threat to oxidative stress [10] and the effect of nickel on human health is pronounced. Knowledge of Ni(II) chemistry towards biologically relevant ligands is crucial. The scarcity of well-characterized materials in the field of pyridoxal-based Schiff bases prompted us to continue research in this direction with Ni(II). The projected ligand can promote binding to a single metal center in a tridentate fashion, thereby making room for another monodentate ligand. This article reports on the syntheses, structural and spectroscopic characterizations, and electrochemical properties of two mononuclear Ni(II) complexes, [Ni(L^1)SCN] (**1**) and [Ni(L^2)SCN] (**2**). A theoretical investigation utilizing density functional theory (DFT) allows rationalization of experimental findings.

2. Experimental

2.1. *Materials and equipment*

All reagents were purchased from Sigma–Aldrich and used as received. Solvents were of analytical grade and used without purification. Elemental (C, H, and N) analyses were performed on a Perkin-Elmer 2400 II analyzer. IR spectra were recorded from 400 to 4000 cm^{-1} on a Bruker-Optics Alpha-T spectrophotometer with samples as KBr disks. Electronic spectra were obtained by using a Hitachi U-3501 spectrophotometer. The luminescence was measured using a LS-55 Perkin-Elmer fluorescence spectrophotometer at room temperature (298 K) in a 1 cm path length quartz cell. Cyclic voltammetric (CV) measurements were done using a BASi Epsilon-EC electrochemical analyzer. The concentration of the supporting electrolyte, tetrabutylammonium perchlorate, was 0.1 M, while that of the complex was 1 mM. CV measurements were carried out in DMF solution at 295 K with a glassy carbon disk working electrode and the scan rate was 50–400 mVs^{-1}.

2.2. *DFT calculations*

The Gaussian 09 software suite was used for all computational modeling [11]. Optimized geometries for **1** and **2** were determined with a DFT method, B3LYP/3–21G(d).

2.3. *Syntheses*

2.3.1. Synthesis of HL^1 and HL^2. HL^1 [((2-(dimethylamino)ethylimino)methyl)-5-(hydroxymethyl)-2-methylpyridin-3-ol] and HL^2 [((2-(diethylamino)ethylimino)methyl)-5-(hydroxymethyl)-2-methylpyridin-3-ol] were synthesized following a common procedure. Details of the synthesis for HL^1 are given below.

Pyridoxal hydrochloride (0.406 g, 2 mM) was dissolved in absolute methanol (15 mL) in the presence of KOH (0.112 g, 2 mM) under stirring. After 1 h of stirring, the separated white solid (KCl) was filtered and the obtained clear solution was added to a solution of N, N-dimethylethylenediamine (0.176 g, 2 mM) (for HL^1) and of N,N-diethylethylenediamine (0.232 g, 2 mM) (for HL^2) in methanol (15 mL) under stirring, and the resulting reaction mixture was refluxed for 4 h. The volume of solvent was reduced to ca. 10 mL and the *in situ* formed yellow–orange ligand was used as such for further reaction. ^{1}H NMR $CDCl_3$: δ 8.90 (s, 1H), 7.74 (s, 1H), 4.72 (s, 1H), 3.78 (t, 2H), 3.42 (s, 1H), 2.69 (t, 2H), 2.46 (s, 3H), 2.30 (s, 6H).

HL^2: ^{1}H NMR $CDCl_3$: δ 8.87(s, 1H), 7.72 (s, 1H), 4.71 (s, 1H), 3.73 (t, 2H), 3.39 (s, 1H), 2.78 (t, 2H), 2.60 (q, 4H), 2.45 (s, 3H), 1.02 (t, 6H).

2.3.2. Synthesis of [Ni(L^1)SCN] (1). To the methanolic solution of 2 mM (0.474 g) of HL^1, a methanolic solution of 2 mM $NiCl_2{\cdot}6H_2O$ (0.475 g) was added dropwise and stirred for 5 min. Then to the resulting green solution, a methanolic solution of 2 mM NH_4SCN (0.152 g) was added. The color of the solution changed from green to red. This resulting solution was stirred for 6 h and then filtered to remove any suspended particles. The clear filtrate was kept undisturbed by standing. The dark red well-formed block shaped single crystals, suitable for X-ray diffraction obtained in 73% yield based on Ni after several weeks, was washed with ether. Anal. Calcd (%) for $C_{13}H_{18}N_4NiO_2S$ (353.07): C, 44.20; H, 5.14; N, 15.87. Found: C, 43.78; H, 5.09; N, 14.31.

2.3.3. Synthesis of [Ni(L^2)SCN] (2). The preparation was carried out with a method similar to that for **1**. The dark red well-formed needle shaped single crystals, suitable for X-ray diffraction obtained in 62% yield based on Ni after several weeks, was washed with ether. Anal. Calcd (%) for $C_{15}H_{22}N_4NiO_2S$ (381.13): C, 47.27; H, 5.84; N, 14.70. Found: C, 46.89; H, 5.72; N, 14.08.

2.4. *X-ray crystallography*

Single crystals of [Ni(L^1)SCN] and [Ni(L^2)SCN] were grown by slow evaporation of methanol solutions at 298 K. Diffraction data were collected on a Nonius APEX-II diffractometer with a CCD-area detector at 293 K using graphite-monochromated Mo Kα radiation ($k = 0.71073$ Å). Crystal structure was determined by direct methods and subsequent Fourier and difference Fourier syntheses, followed by full-matrix least-squares refinements on F^2 using SHELXL-97 and SHELXL-2013 [12]. Absorption correction was done by SADABS. Hydrogens were located and refined freely. Hydrogens were refined isotropically, while the non-hydrogen atoms were refined anisotropically.

3. Results and discussion

3.1. *Syntheses and characterization*

The interaction of a methanolic solution of $NiCl_2{\cdot}6H_2O$ with HL^1/HL^2 in the presence of NH_4SCN afforded dark red crystals of **1** and **2**, respectively (scheme 1). The isolated complexes were characterized by IR and UV–vis spectroscopy, CV, and by single-crystal X-ray crystallography. Both complexes are air stable.

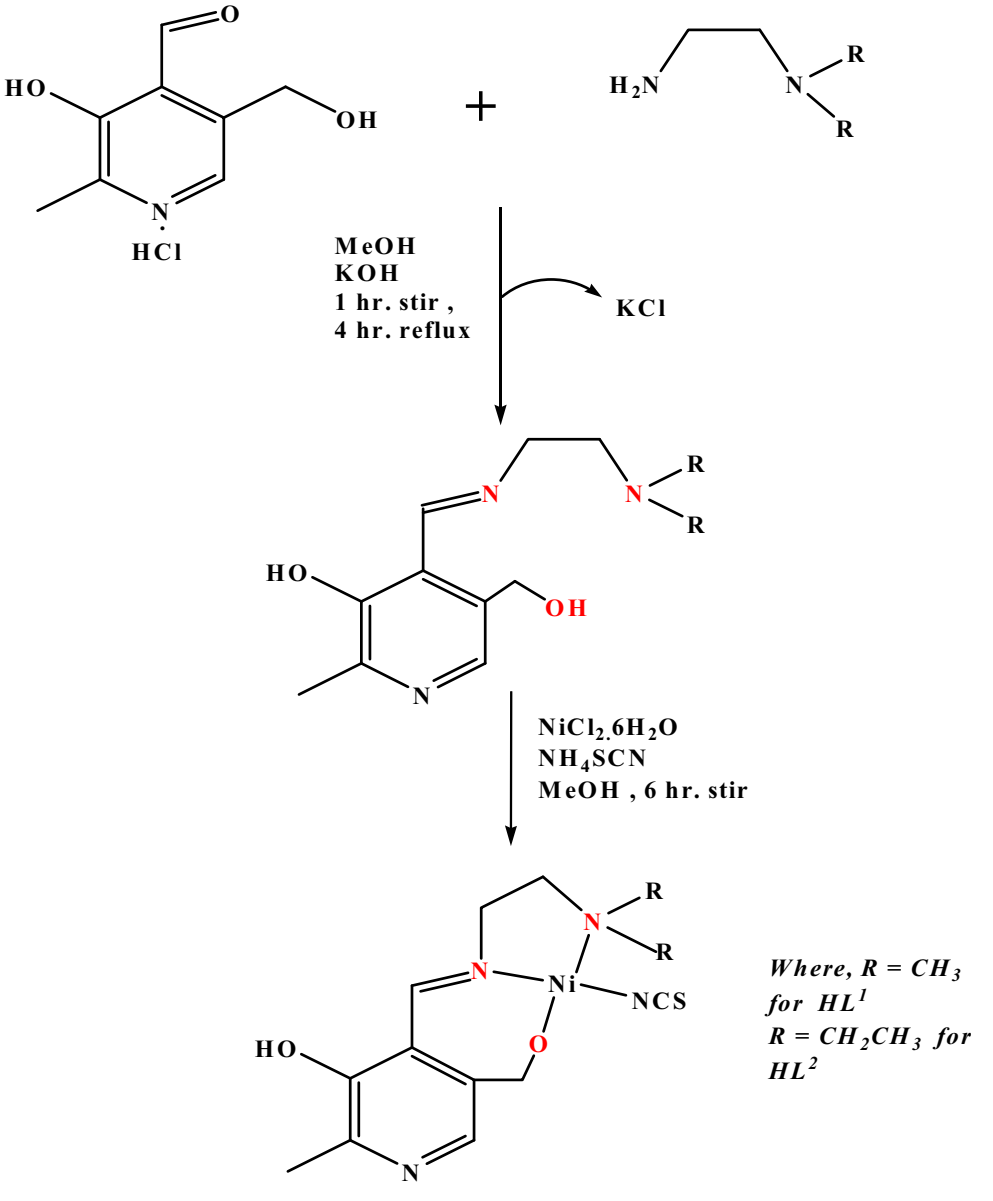

Scheme 1. Schematic illustration of preparation of ligands and their Ni(II) complexes.

3.2. *Characterization*

3.2.1. UV–vis spectra. The electronic absorption spectra of both **1** and **2**, recorded in UV-grade DMF, are shown in figure S1 (see online supplemental material at http://dx.doi.org/10.1080/00958972.2014.890190). The absorption bands at 416 and 388 nm are assigned to the $^1A_{1g} \rightarrow {}^1B_{1g}$ transition for a square planar Ni(II) species. The absorptions at 844 and 874 nm can be assigned to the $^1A_{1g} \rightarrow {}^1A_{2g}$ transition. The electronic spectra in the solid state (figure S2) taken in Nujol mull reveals the presence of two distinct bands at 466 and 796 nm (for **1**) and 410 and 811 nm (for **2**), which are in accord with the spectral data obtained for the solution phase [13].

3.2.2. Infrared spectra. IR spectra of **1** and **2** (figure S3) display a very strong absorption around 2043 and 2117 cm^{-1}, respectively, due to ν_{as}(C≡N) of the coordinated isothiocyanate [14–18]. The preference of the divalent first-row transition metal ions to coordinate to the thiocyanate N instead of S is well documented and usually explained in terms of their hard (N) and soft (S) character [19]. Complexes **1** and **2** also display a broad band of medium intensity at 3222 and 3355 cm^{-1}, respectively, attributed to the –OH stretching vibration of the $–CH_2OH$ of the pyridoxal part of the ligand. A moderately sharp band around 1617 cm^{-1} for both the complexes is assigned as stretching vibration of the azomethine (C=N).

3.2.3. ^{1}H NMR spectra. HL^1 and HL^2 were characterized by ^{1}H NMR spectra and the data are given in the experimental section (figure S4). The azomethine protons in HL^1 and HL^2 are sharp singlets at 8.90 and 8.87 ppm, respectively. A sharp singlet at 7.75 and 7.72 ppm for HL^1 and HL^2, respectively, is assigned as the proton ortho to nitrogen of the pyridine ring. Another sharp singlet at 4.72 and 4.71 ppm for HL^1 and HL^2, respectively, is assigned as the proton attached to carbon of the $–CH_2OH$ moiety. A triplet at 3.78 and 3.73 ppm for HL^1 and HL^2, respectively, is assigned to the two protons attached to the carbon which is further attached to the azomethine nitrogen. Another sharp singlet at 3.42 and 3.39 ppm for HL^1 and HL^2, respectively, is assigned as the proton attached to oxygen of $–CH_2OH$. Another triplet at 2.69 and 2.70 ppm for HL^1 and HL^2, respectively, is assigned as the two protons attached to carbon near the tertiary nitrogen of amine. A strong sharp singlet at 2.45 ppm is due to the three protons of $–CH_3$ attached to the ortho position with respect to nitrogen of pyridine. For HL^1, we observed a sharp singlet at 2.30 ppm for two methyl hydrogens of the end nitrogen of amine, whereas for HL^2, one quartet at 2.60 ppm and one singlet at 1.02 ppm clearly indicate the presence of $–CH_2CH_3$ attached to the tertiary nitrogen of the amine for both cases. Peaks for the phenolic proton are absent probably due to rapid exchange of deuterium of $CDCl_3$.

3.3. *Description of crystal structures*

Compound **1** crystallizes in the monoclinic space group *C2/c*. The relevant crystal data and structural refinement parameters are presented in table 1. The asymmetric unit contains one crystallographically independent Ni(II), one HL^1, and one thiocyanate. As depicted in figure 1, Ni1 is surrounded by a N_3O ligand environment to give a slightly distorted square planar geometry. The coordination sites are occupied by phenoxo O2, imine N2, and amine N1 of the Schiff base and the remaining position contains an isothiocyanate (N4). The

Table 1. Summary of crystal data, data collection, structure, and refinement details for **1** and **2**.

Parameters	**1**	**2**
Empirical formula	$C_{13}H_{18}N_4NiO_2S$	$C_{15}H_{22}N_4NiO_2S$
Mr	353.07	381.13
Temp/K	296(2)	296(2)
Crystal system	Monoclinic	Triclinic
Space group	*C2/c*	*P-1*
a/Å	14.5525(4)	6.8146(13)
b/Å	10.9871(3)	8.7463(18)
c/Å	17.9459(5)	14.996(3)
α/°	90	100.638(10)
β/°	92.667(10)	100.735(10)
γ/°	90	101.430(6)
V/Å^3	2866.26(14)	837.7(3)
Z	8	2
D_{Calcd}/g cm^{-3}	1.557	1.515
μ/mm^{-1}	1.506	1.297
Reflections collected	17925	7100
Independent reflections	2446	2667
R_{int}	0.023	0.021
R_1 [$I > 2\sigma(I)$][a]	0.0612	0.0633
wR_2 [$I > 2\sigma(I)$]	0.1803	0.2167
Goodness of fit on F^2	1.064	1.108

[a] $R_1 = \Sigma(||F_0| - |F_c||)/\Sigma|F_0|$; $wR_2 = [\Sigma w(F_0^2 - F_c^2)^2/\Sigma w(F_0^2)^2]^{1/2}$.

deviations of the basal N1, N2, O2, and N4 from the least-square mean plane are −0.007, −0.002, −0.007, and 0.002 Å, respectively. Ni1 is displaced 0.010 Å above the mean plane. The Ni1–O2 bond length is 1.835 Å, whereas the Ni–N bond lengths are 1.9 Å [table 2(a)] (Ni1–N1 = 1.953 Å, Ni1–N2 = 1.848 Å, Ni1–N4 = 1.897 Å, falling within the normal range) [20–25]. Yang *et al*. defined a four-coordinate geometry index, τ_4, to quantitatively ascertain the geometry of a four-coordinate complex [26]. They proposed a very simple geometry index, $\tau_4 = [360° - (\alpha + \beta)]/141°$. It is the sum of angles α and β—the two largest angles in the four-coordinate species, subtracted from 360°, all divided by 141°. The values of τ_4 will

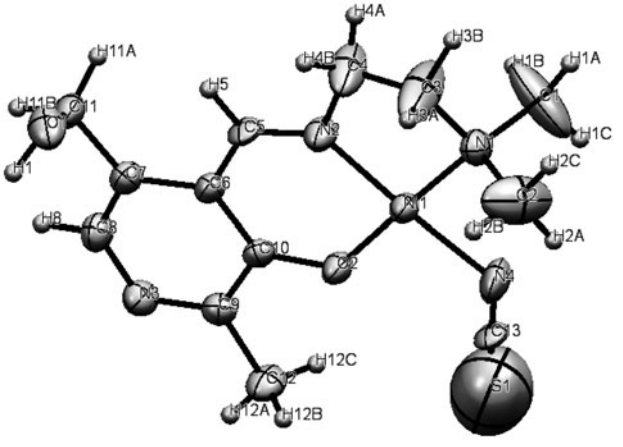

Figure 1. ORTEP representation of **1**.

Table 2. (a). Selected bond distances (Å) and angles (°) for **1**.

Bond lengths	
Ni1–O2	1.835(3)
Ni1–N1	1.953(4)
Ni1–N2	1.848(4)
Ni1–N4	1.897(5)
Bond angles	
O2–Ni1–N1	178.60(16)
O2–Ni1–N2	94.27(16)
O2–Ni1–N4	89.95(18)
N1–Ni1–N2	86.70(18)
N1–Ni1–N4	89.1(2)
N2–Ni1–N4	175.7(2)

Table 2. (b). Selected bond distances (Å) and angles (°) for **2**.

Bond lengths	
Ni1–O1	1.848(3)
Ni1–N2	1.844(4)
Ni1–N3	1.998(4)
Ni1–N4	1.885(5)
Bond angles	
O1–Ni1–N2	93.69(17)
O1–Ni1–N3	178.55(18)
O1–Ni1–N4	86.42(17)
N2–Ni1–N3	86.49(19)
N2–Ni1–N4	179.7(2)
N3–Ni1–N4	93.40(19)

range from 1.00 for a perfect tetrahedral geometry, since $360 - 2(109.5) = 141$, to zero for a perfect square planar geometry, since $360 - 2(180) = 0$. Intermediate structures, including trigonal pyramidal and seesaw, fall within the range of 0–1.00. Complex **1** has a τ_4 value of 0.04 ($\alpha = \angle$O2–Ni1–N1 = 178.60(16)° and $\beta = \angle$N2–Ni1–N4 = 175.7(2)°) supporting an

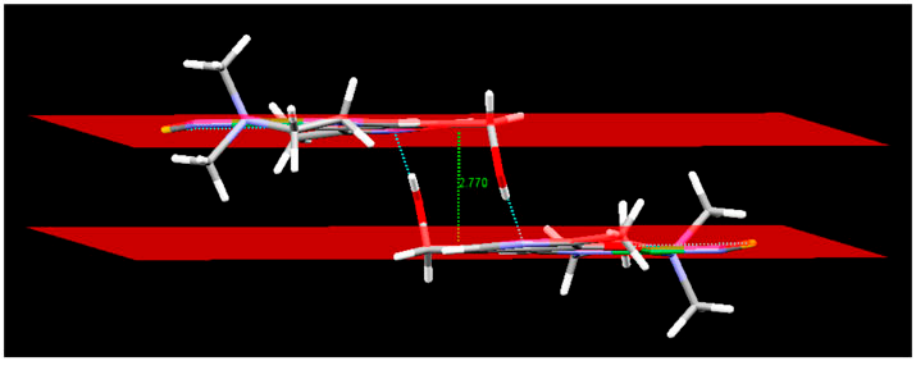

Figure 2(a). Hydrogen bonded dimeric entity showing the separation between the mean planes in **1**.

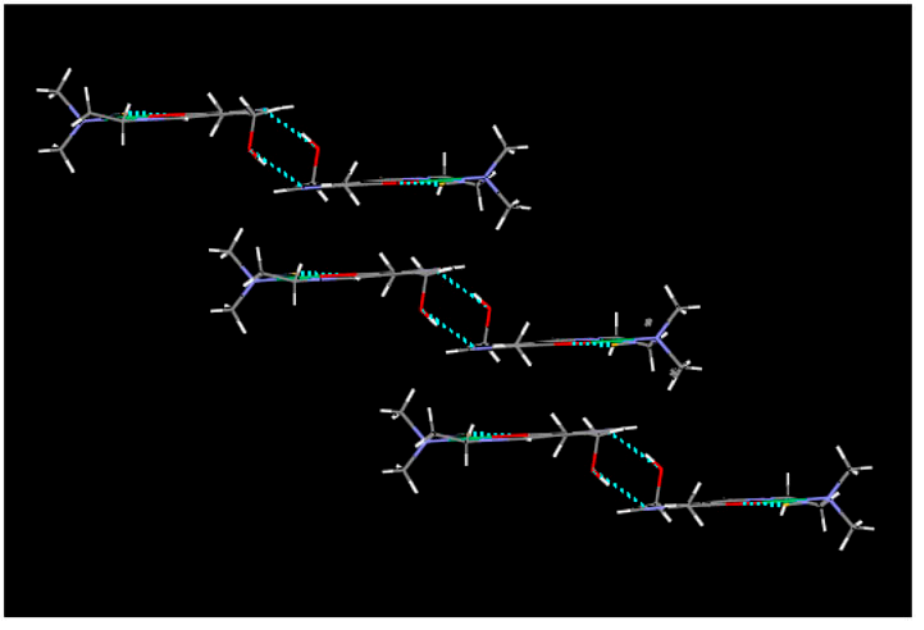

Figure 2(b). Offset parallel fashion of dinuclear units of **1**, stacked by adjacent H-bonds and weak van der Waal's interaction.

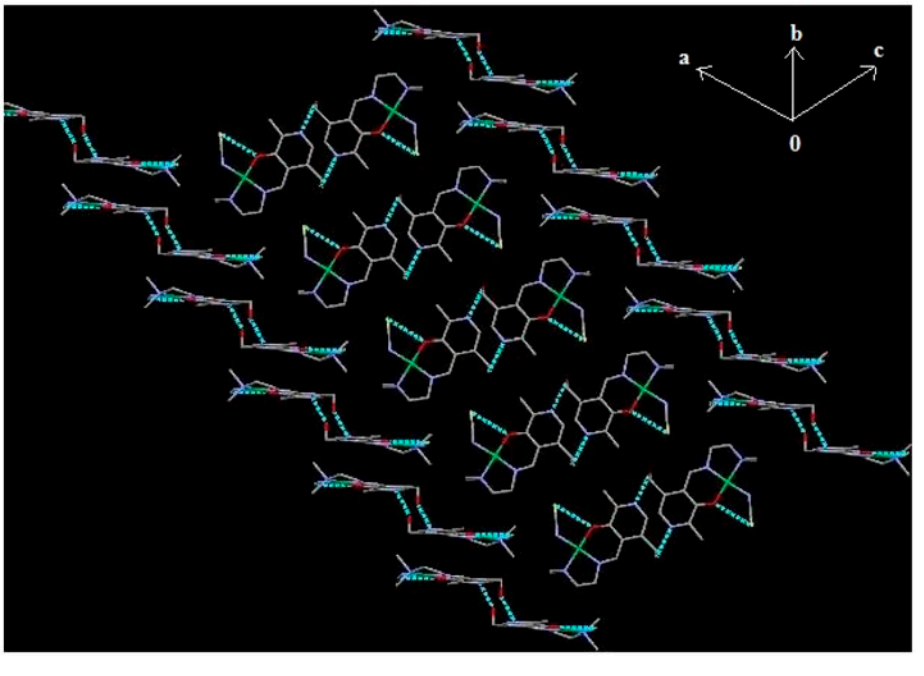

Figure 2(c). Stacking of dinuclear unit in slightly offset parallel fashion in **1**.

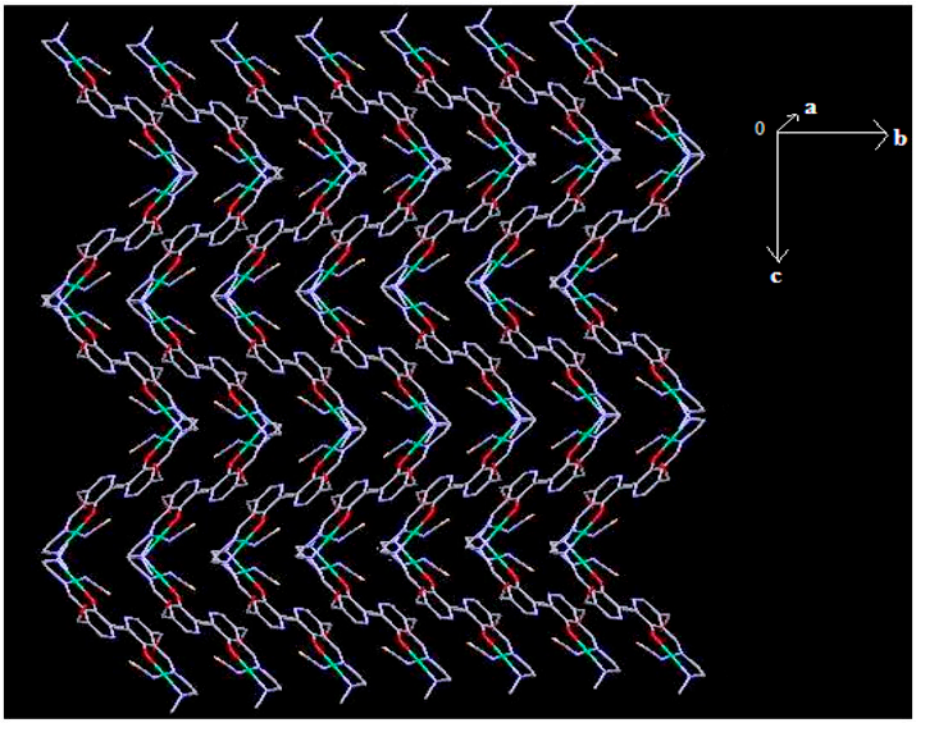

Figure 2(d). 3-D supramolecular framework having corrugated sheet-like pattern of **1**.

assignment of slightly distorted square planar geometry around nickel. The almost linear conformation of the isothiocyanate shows a N–C–S angle of 176.17°. A large bending is observed at N4 with a Ni1–N4–C13 angle of 124.05° [27–30]. A very weak intramolecular

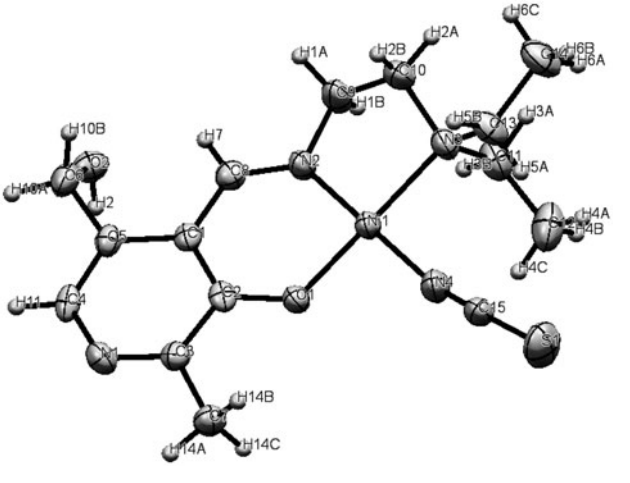

Figure 3. ORTEP representation of **2**.

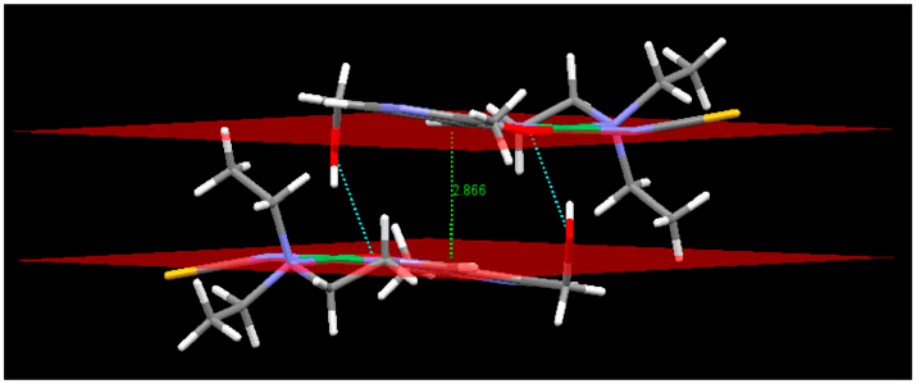

Figure 4(a). Hydrogen bonded dimeric entity showing the separation between the mean planes in **2**.

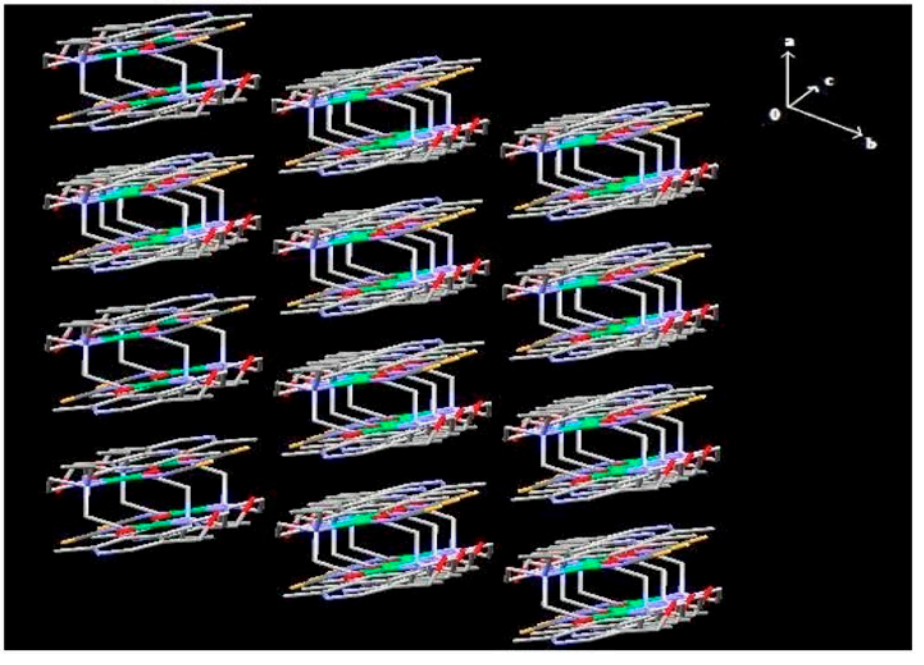

Figure 4(b). Column-like stacking of dimeric unit generating a 3-D supramolecular architecture in **2**.

sulfur-oxygen interaction is observed in the crystal packing with a S1···O2 distance of 3.212 Å.

The uncoordinated pyridine and oxygen of the $-CH_2OH$ group actively participate in hydrogen bonding interaction (O1–H1···N3 = 2.868(6) Å), leading to a hydrogen bonded pseudo-dimeric entity [figure 2(a)] with a Ni···Ni distance of 12.183 Å and mean plane

separation of 2.770 Å. The adjacent H-bonded dinuclear units stack in a slightly offset parallel fashion through weak van der Waal's interaction [figure 2(b)]. There is another such parallel form oriented slightly tilted from the previous one [figure 2(c)]. Therefore, the overall packing diagram exhibits a 3-D supramolecular framework having a corrugated sheet-like pattern [figure 2(d)].

The single-crystal analysis reveals that **2** crystallizes in triclinic space group *P-1*. The relevant crystal data and structural refinement parameters are presented in table 1. The local coordination geometry around Ni^{2+} is depicted in figure 3. Ni1 coordinates to one phenoxo oxygen (O1), one imine nitrogen (N2), and an amine nitrogen (N3) from the ligand, whereas the fourth position is occupied by the isothiocyanate (N4), resulting in a slightly distorted square planar structure. The deviations of the basal coordinating atoms N2, N3, O1, and N4 from the least-square mean plane through them are 0.007, −0.012, 0.013, and 0.006 Å, respectively. Ni1 is displaced 0.012 Å above the mean plane. The value of the τ_4 index is 0.013 for **2**. The Ni–O bond length is 1.848 Å and the Ni–N lengths are 1.844 and 1.998 Å, which are similar to the values found in other Ni(II) complexes [table 2(b)] [20–25]. The isothiocyanate is practically linear with a N–C–S angle of 177.86°. Unlike **1**, here the departure from the strict linearity of the ∠Ni1–N4–C15 fragment is small (167.78°).

Hydrogen bonding also plays an essential role in generating the dimeric entity through O–H···O interactions (O2–H2···O1 = 2.917 Å) involving the phenoxo oxygen and the $-CH_2OH$ group. The Ni···Ni distance in the dimer is 6.704 Å, whereas the mean plane separation is 2.866 Å [figure 4(a)]. These dimeric units are further stacked in segregated columns by weak van der Waal's interaction generating a 3-D supramolecular architecture [figure 4(b)].

1 and **2** are comparable with other reported Ni(II) complexes of various Schiff base ligands with a N_2O environment [31].

3.4. *Electrochemical measurements*

The electrochemical properties of the complexes were studied by CV in DMF at 295 K using a glassy carbon disk working electrode (figure 5). The cyclic voltammogram of **1** displays an electrochemically irreversible reduction at $E_{1/2} = -1.72$ V and a facile oxidation at $E_{1/2} = -0.618$ V attributable to the Ni^{II}/Ni^{I} and Ni^{II}/Ni^{III} couples, respectively. Complex **2** exhibits irreversible reduction at $E_{1/2} = -1.59$ V and oxidation at $E_{1/2} = +0.52$ V, which may be assigned to Ni^{II}/Ni^{I} and Ni^{II}/Ni^{III} couples, respectively. The $E_{1/2}$ values remain almost the same on variation of the scan rate (50–400 mVs^{-1}) [32].

3.5. *Fluorescence spectra*

The fluorescence spectra of HL^1 and HL^2 were obtained by excitation at 411 and 334 nm, respectively, in methanol. In the absence of a metal ion, a strong emission was observed at 472 nm and 438 nm, respectively, which are assigned to the intraligand (π–π^*) transitions. On addition of Ni(II), the fluorescence intensity of HL^1 was diminished to some extent but no red shift was observed with respect to the emission peak of the ligand. For HL^2, the emission intensity remained unchanged on addition of Ni(II) (figure S5) [33].

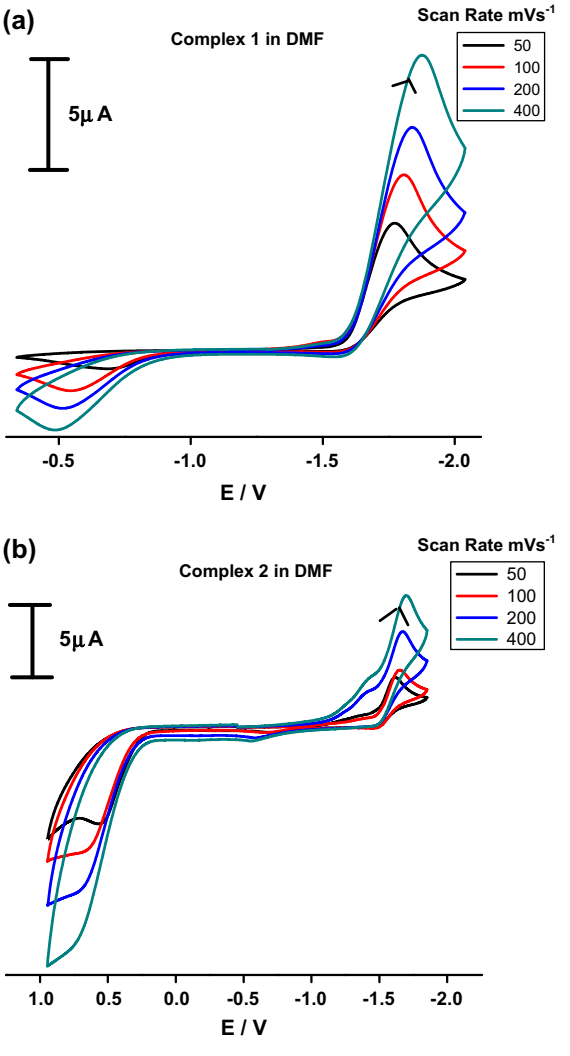

Figure 5. (a) Cyclic voltammogram of **1** and (b) cyclic voltammogram of **2** in DMF.

3.6. *Theoretical investigations*

The geometry optimization was performed for both complexes and the data of energy minimization showed that **1** and **2** are stabilized by −75298.28 and −77415.45 eV, respectively, indicating that they are stable and their electronic structures are similar (figure S6). The forms of the HOMO and LUMO wave functions are given in figures 6 and 7. The plot of the highest occupied molecular orbitals or HOMOs of **1** and **2** indicate that the HOMOs are delocalized and reside mainly on the orbitals of Ni(II), the isothiocyanate, and partially on the pyridoxal unit of the Schiff base. The LUMOs are comparatively less localized and spread over the orbitals of the entire pyridoxal fragment and Ni(II). The HOMO–LUMO gap of 2.8717 and 2.8775 eV is consistent with the experimental observation that **1** and **2** have very similar absorption and photoluminescence spectral output.

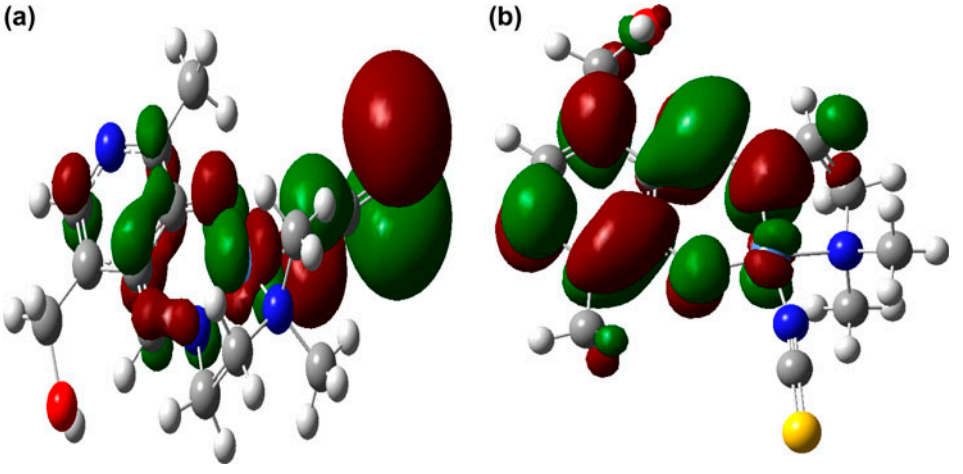

Figure 6. Surface plots of (a) HOMO and (b) LUMO of **1**.

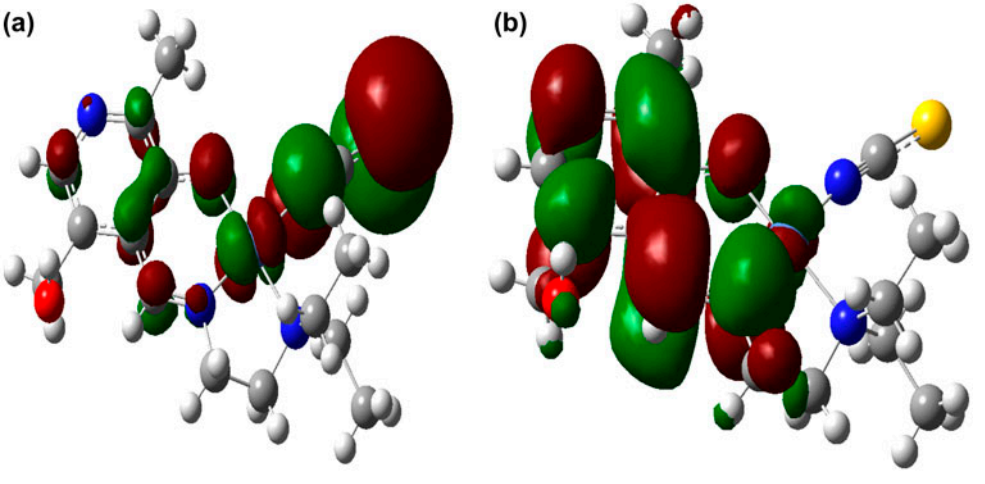

Figure 7. Surface plots of (a) HOMO and (b) LUMO of **2**.

4. Conclusion

Two ONN donor pyridoxal derived Schiff base Ni(II) complexes have been synthesized and characterized in detail by X-ray crystallography, electrochemistry, and photo-physical studies. Structural investigations reveal slightly distorted square planar geometry around Ni(II) with different angle of coordination of the isothiocyanate nitrogen to Ni(II). These compounds exhibit irreversible Ni^{II}/Ni^{I} reduction and Ni^{II}/Ni^{III} oxidation couples in DMF. Single-point DFT calculations showed that the electronic structure of the complexes and photo-physical output are very similar.

Supplementary material

Figures S1–S6 show the UV/Vis, FT-IR, ^{1}H NMR, emission spectra, and geometry optimized structures of ligands and complexes. CCDC Nos. 950997–950998 (**1** and **2**) contain the supplementary crystallographic data. These data can be obtained free of charge via the Cambridge Crystallographic Data Center (e-mail: deposit@ccdc.cam.ac.uk; website: http://www.ccdc.cam.ac.uk/deposit).

Acknowledgements

We thank DST for a junior research fellowship to Sikdar [sanction no. SR/FT/CS-107/2011]. DST-FIST is acknowledged for providing the X-ray diffraction facility at the Department of Chemistry, University of Calcutta.

Funding

Financial support from the University Grants Commission for a junior research fellowship to Mandal [sanction no. UGC/749/Jr. fellow(Sc.)] and a RFSMS fellowship [sanction no. UGC/740/RFSMS] to Modak are gratefully acknowledged.

References

[1] A.C. Eliot, J.F. Kirsch. *Annu. Rev. Biochem.*, **73**, 383 (2004).
[2] R.A. John. *Biochim. Biophys. Acta*, **1248**, 81 (1995).
[3] M.D. Toney. *Arch. Biochem. Biophys.*, **433**, 279 (2005).
[4] E.E. Snell. *J. Am. Chem. Soc.*, **67**, 194 (1945).
[5] M. Strianese, S. Milione, A. Maranzana, A. Grassi, C. Pellecchia. *Chem. Commun.*, **48**, 11419 (2012).
[6] I. Correia, J.C. Pessoa, M.T. Duarte, R.T. Henriques, M.F. Piedade, L.F. Veiros, T. Jakusch, T. Kiss, A. Dörnyei, M.M. Castro, C.F. Geraldes, F. Avecilla. *Chem. Eur. J.*, **10**, 2301 (2004).
[7] S. Mandal, R. Modak, S. Goswami. *J. Mol. Struct.*, **1037**, 352 (2013).
[8] H. Adams, S. Clunas, D.E. Fenton, S.E. Spey. *J. Chem. Soc., Dalton Trans.*, 441 (2002).
[9] A. Sigel, H. Sigel, R.K.O. Sigel (Eds.). *Metal Ions in Life Sciences: Nickel and Its Surprising Impact in Nature*, Vol. 2, Wiley, New York (2007).
[10] K.K. Das, S.N. Das, S.A. Dhundasi. *Indian J. Med. Res.*, **128**, 412 (2008).
[11] M.J. Frisch, G.W. Trucks, H.B. Schlegel, G.E. Scuseria, M.A. Robb, J.R. Cheeseman, G. Scalmani, V. Barone, B. Mennucci, G.A. Petersson, H. Nakatsuji, M. Caricato, X. Li, H.P. Hratchian, A.F. Izmaylov, J. Bloino, G. Zheng, J.L. Sonnenberg, M. Hada, M. Ehara, K. Toyota, R. Fukuda, J. Hasegawa, M. Ishida, T. Nakajima, Y. Honda, O. Kitao, H. Nakai, T. Vreven, J.A. Montgomery Jr, J.E. Peralta, F. Ogliaro, M. Bearpark, J.J. Heyd, E. Brothers, K.N. Kudin, V.N. Staroverov, T. Keith, R. Kobayashi, J. Normand, K. Raghavachari, A. Rendell, J.C. Burant, S.S. Iyengar, J. Tomasi, M. Cossi, N. Rega, J.M. Millam, M. Klene, J.E. Knox, J.B. Cross, V. Bakken, C. Adamo, J. Jaramillo, R. Gomperts, R.E. Stratmann, O. Yazyev, A.J. Austin, R. Cammi, C. Pomelli, J.W. Ochterski, R.L. Martin, K. Morokuma, V.G. Zakrzewski, G.A. Voth, P. Salvador, J.J. Dannenberg, S. Dapprich, A.D. Daniels, O. Farkas, J.B. Foresman, J.V. Ortiz, J. Cioslowski, D.J. Fox. *Gaussian 09, Revision B.01*, Gaussian Inc, Wallingford, CT (2010).
[12] (a) G.M. Sheldrick. *SHELXL-97*, Crystal Structure Refinement Program, University of Göttingen, Göttingen (1997); (b) G.M. Sheldrick. *SHELXL-2013*, Crystal Structure Refinement Program, University of Göttingen, Göttingen (2013).
[13] (a) A.B.P. Lever. *Inorganic Electronic Spectroscopy*, Elsevier, Amsterdam, **513**, (1984); (b) A. la Cour, M. Findeisen, R. Hazell, L. Hennig, C.E. Olsen, O. Simonsen. *J. Chem. Soc., Dalton Trans.*, (1996).
[14] (a) F.A. Mautner, J.H. Albering, R. Vicente, F.R. Louka, A.A. Gallo, S.S. Massoud. *Inorg. Chim. Acta*, **365**, 290 (2011); (b) U. Mukhopadhyay, I. Bernal, S.S. Massoud, F.A. Mautner. *Inorg. Chim. Acta*, **357**, 3673 (2004).

[15] F.A. Mautner, F.R. Louka, A.A. Gallo, J.H. Albering, M.R. Saber, N.B. Burham, S.S. Massoud. *Transition Met. Chem.*, **35**, 613 (2010).
[16] F.A. Mautner, R. Vicente, S.S. Massoud. *Polyhedron*, **25**, 1673 (2006).
[17] S.S. Massoud, F.A. Mautner. *Inorg. Chim. Acta*, **358**, 3334 (2005).
[18] K. Nakamoto. *Infrared and Raman Spectra of Inorganic and Coordination Compounds*, 5th Edn, Wiley, New York (1997).
[19] P. Atkins, T. Overton, J. Rourke, M. Weller, F. Armstrong. *Shriver & Atkins' Inorganic Chemistry*, 5th Edn, Oxford University Press, Oxford (2010).
[20] M.D. Santana, R. García-Bueno, G. García, J. Pérez, L. García, M. Monge, A. Laguna. *Dalton Trans.*, 1797 (2010).
[21] B.M. Kukovec, P.D. Vaz, M.J. Calhorda, Z. Popović. *Polyhedron*, **39**, 66 (2012).
[22] J.P. Wikstrom, A.S. Filatov, E.A. Mikhalyova, M. Shatruk, B.M. Foxman, E.V. Rybak-Akimova. *Dalton Trans.*, 2504 (2010).
[23] R. García-Bueno, M.D. Santana, G. Sánchez, J. García, G. García, J. Pérez, L. García. *Dalton Trans.*, 5728 (2010).
[24] M.D. Santana, G. García, J. Pérez, E. Molins, G. López. *Inorg. Chem.*, **40**, 5701 (2001).
[25] M.D. Santana, G. García, G. López, A. Lozano, C. Vicente, L. García, J. Pérez. *Polyhedron*, **26**, 1029 (2007).
[26] L. Yang, D.R. Powell, R.P. Houser. *Dalton Trans.*, (2007).
[27] T.V. Brinzari, C. Tian, G.J. Halder, J.L. Musfeldt, M.-H. Whangbo, J.A. Schlueter. *Inorg. Chem.*, **48**, 7650 (2009).
[28] A. Biswas, L.K. Das, M.G.B. Drew, G. Aromí, P. Gamez, A. Ghosh. *Inorg. Chem.*, **51**, 7993 (2012).
[29] L.M. Callejo, N. de la Pinta, G. Madariaga, L. Fidalgo, L. Lezama, R. Cortés. *Cryst. Growth Des.*, **10**, 4874 (2010).
[30] J.M. Clemente-Juan, B. Chansou, B. Donnadieu, J.-P. Tuchagues. *Inorg. Chem.*, **39**, 5515 (2000).
[31] (a) A. Das, S. Shit, M. Köckerling, A.S. Batsanov, S. Mitra. *J. Coord. Chem.*, **66**, 2587 (2013); (b) K.A. Siddiqui. *J. Coord. Chem.*, **66**, 2039 (2013); (c) X. Qiu, J. Wang, D. Shi, S. Li, F. Zhang, F. Zhang, G. Cao, B. Zhai. *J. Coord. Chem.*, **66**, 1616 (2013); (d) S.M. Saadeh. *J. Coord. Chem.*, **65**, 3075 (2012); (e) R. Rajarao, T.H. Kim, B.R. Bhat. *J. Coord. Chem.*, **65**, 2671 (2012); (f) R.N. Patel, A. Singh, V.P. Sondhiya, Y. Singh, K.K. Shukla, D.K. Patel, R. Pandey. *J. Coord. Chem.*, **65**, 795 (2012); (g) Y. Lu, D.-H. Shi, Z.-L. You, X.-S. Zhou, K. Li. *J. Coord. Chem.*, **65**, 339 (2012).
[32] (a) B. Castro, C. Freire. *Inorg. Chem.*, **29**, 5113 (1990); (b) S. Sen, C.R. Choudhury, P. Talukder, S. Mitra, M. Westerhausenb, A.N. Kneifel, C. Desplanches, N. Daro, J.-P. Sutter. *Polyhedron*, **25**, 1271 (2006); (c) E. Pereira, L. Gómez, B. Castro. *Inorg. Chim. Acta*, **271**, 83 (1998); (d) M. Cañadas, E. López-Torres, A. Martínez-Arias, M.A. Mendiola, M.T. Sevilla. *Polyhedron*, **19**, 2059 (2000); (e) A.J. Blake, R.O. Gould, M.A. Halcrow, M. Schröeder. *J. Chem. Soc., Dalton Trans.*, (1993).
[33] (a) N.J. Turro. *Pure Appl. Chem.*, **49**, 3071 (1977); (b) Y.H. Xing, J. Han, G.H. Zhou, Z. Sun, X.J. Zhang, B.L. Zhang, Y.H. Zhang, H.Q. Yuan, M.F. Ge. *J. Coord. Chem.*, **61**, 715 (2008); (c) J.-M. Lin, W.-B. Chen, X.-M. Lin, A.-H. Lin, C.-Y. Ma, W. Dong, C.-E. Tian. *Chem. Commun.*, **47**, 2402 (2011); (d) T. Chattopadhyay, M. Mukherjee, K.S. Banu, A. Banerjee, E. Suresh, E. Zangrando, D. Das. *J. Coord. Chem.*, **62**, 967 (2009); (e) H.-J. Son, W.-S. Han, J.-Y. Chun, B.-K. Kang, S.-N. Kwon, J. Ko, S.J. Han, C. Lee, S.J. Kim, S.O. Kang. *Inorg. Chem.*, **47**, 5666 (2008).